

# Edge-aware Hard Clustering Graph Pooling for Brain Imaging Data

Cheng Zhu<sup>#1</sup>, Jiayi Zhu<sup>#2</sup>, Lijuan Zhang<sup>1</sup>, Xi Wu<sup>1</sup>, Shuqi Yang<sup>1</sup>, Ping Liang<sup>1</sup>, Honghan Chen<sup>1</sup>, Ying Tan<sup>\*1</sup>

<sup>1</sup>The Key Laboratory for Computer Systems of State Ethnic Affairs Commission, Southwest Minzu University, Chengdu, 610041, China

<sup>2</sup>State Key Laboratory of Cognitive Neuroscience and Learning, Beijing Normal University, Beijing 100875, China  
190852112021@stu.swun.edu.cn, zhujiayii0102@163.com, 220854112016@stu.swun.edu.cn, 13769472963@163.com, ysqwymail@163.com, 21700059@swun.edu.cn, honghanchen@hotmail.com, ty7499@swun.edu.cn

## Abstract

Graph Convolutional Networks (GCNs) can capture non-Euclidean spatial dependence between different brain regions, and the graph pooling operator in GCNs is key to enhancing the representation learning capability and acquiring abnormal brain maps. However, the majority of existing research designs graph pooling operators only from the perspective of nodes while disregarding the original edge features, in a way that not only confines graph pooling application scenarios, but also diminishes its ability to capture critical substructures. In this study, a clustering graph pooling method that first supports multidimensional edge features, called Edge-aware hard clustering graph pooling (EHCPool), is developed. EHCPool proposes the first ‘Edge-to-node’ score evaluation criterion based on edge features to assess node feature significance. To more effectively capture the critical subgraphs, a novel Iteration n-top strategy is further designed to adaptively learn sparse hard clustering assignments for graphs. Subsequently, an innovative N-E Aggregation strategy is presented to aggregate node and edge feature information in each independent subgraph. The proposed model was evaluated on multi-site brain imaging public datasets and yielded state-of-the-art performance. We believe this method is the first deep learning tool with the potential to probe different types of abnormal functional brain networks from data-driven perspective. Core code is at: <https://github.com/swfen/EHCPool>.

## Introduction

The brain can be regarded as a complex graph structure in non-Euclidean space. Because graph convolutional networks (GCNs) are one of the few advanced deep learning methods that can directly analyze graph structures, many studies have explored the brain using GCNs in recent years. For example, Hi-GCN (Jiang et al. 2020) jointly learns graph embeddings from individual brain network structures and correlations among subjects. M-GCN (Dsouza et al. 2021) utilizes the anatomical pathways to learn feature representations from brain functional connectivity. MVS-GCN (Wen et al. 2022) combines graph structure learning with multi-task graph embedding to identify potential brain func-

tional networks. The aforementioned studies all utilized innovative GCNs frameworks or sophisticated graph convolution methods to explore brain activities and have demonstrated enhancements in model accuracy. However, in graph-level classification tasks, an elaborate graph pooling operator occupies an indispensable role in learning abstract representations of the brain. Since Graph pooling has not been extensively studied (Zhang et al.2023), and is tailored to the brain image data characteristics is nascent. Therefore, it is important to design advanced graph pooling operators based on specific data scenarios.

Nowadays, GCNs research rarely focuses on edge features. However, a similar situation exists in all types of complex systems and graph problems (e.g., brain image analysis, path selection, and recommendation system), where the importance or utilization of edge information may be more significant than that of node information. Take the brain imaging problem as an example, functional Magnetic Resonance Imaging (fMRI) is the mainstream detection technology used to explore the functional activities of the brain (Huettel 2012; Lin et al.2016). Among them, the functional connectivity (FC), that is, the correlation of activities in different brain regions, is one of the most exploited and classically versatile features (Bifone, Gozzi, and Schwarz 2010; Nili et al. 2023). In the graph structure, brain regions are used as nodes and FC between brain regions as edges, which is in line with the logical structure of brain data, and has been widely recognized (Li et al. 2019; Li et al. 2021). However, owing to a lack of reasonable use and evaluation methods for edge information in the graph, many studies based on fMRI have utilized GCNs by assigning logical edge information (i.e., FC) directly to the graph nodes which does not design edge information (Venkatapathy et al. 2023; Klepl et al. 2022; Pitsik et al. 2023), resulting in the loss of structural representations of the graphs. Thus, graph pooling operators targeted at dominant edge features are beneficial for overcoming the current technical bottlenecks to achieve higher model performance.

---

<sup>#</sup> These authors contributed equally to this work

<sup>\*</sup> Corresponding Author

On the other hand, almost all emerging graph clustering methods have used soft clustering (a node belongs to more than one cluster). For example, AHDDC (Dong et al. 2023) uses attention-based soft clustering method to strengthen the structural information. AGCC (He et al. 2022) is an end-to-end parallel adaptive soft clustering model to propagate optimal data representations. Learnable Pooling (Gopinath et al. 2022) proposed a soft clustering approach that learn the intrinsic aggregation of nodes based on graph embedding. Most methods use clustering to classify nodes into different subgraphs (clusters) and subsequently aggregate the information from each subgraph into corresponding basis vectors for training to exclude data redundancy or aggregate high-value feature information. However, these soft clustering approaches are highly likely to cause different subgraphs basis vectors to repeatedly focus on individual high-value (highly abnormal) node information, rather than enabling the model to adaptively discover more critical subgraphs with differentiation, thus reducing the interpretability of the model (Zhang et al. 2023; Wagner et al. 2022).

To overcome the limitations of existing graph pooling operators as well as to adapt the brain fMRI data characteristics, we propose a clustering graph pooling method that first supports multidimensional edge features called edge-aware hard clustering graph pooling (EHCPool). Detailedly, EHCPool initially presents an edge feature score criterion, which evaluates the importance of edge features in an adaptive manner, and subsequently obtains the corresponding target node scores using an Edge-to-node strategy. Thereafter, based on the score ranking of all nodes, the most informative node is selected as the core node (cluster center) of the current subgraph (cluster) in order using the Iteration n-top strategy. And with each core node as the center, a finite number of neighborhood nodes that have maximal neighboring edge scores are selected to form the corresponding subgraphs. Finally, the N-E aggregation aggregates the subgraph vicinity information to the core node, which in turn forms the basis vector representing each subgraph for the output. In addition, Table 1 shows a comparison of the properties of different graph pooling operators with EHCPool, including Top-kPool (Gao and Ji 2019), SAGPool (Lee, Lee, and Kang 2019), DiffPool (Ying et al. 2018) and ASAP (Ranjan, Sanyal, and Talukdar 2019), from which it can be observed that EHCPool consists of additional properties.

In summary, EHCPool provides a novel application concept for GCNs data problems, where the importance of edge features is greater than that of node features. The principal contributions can be outlined as follows:

- The first feature evaluation criterion is proposed for measuring the significance of nodes based on edge feature information scores: Edge-to-node. This strategy estab-

lishes a connection between nodes and edge feature information, and holistically considers both global and local representations.

- A subgraph acquisition strategy is presented utilizing adaptive sparse hard clustering: Iteration n-top. This strategy avoids duplicate representations of individual high-value information across different subgraphs and has the potential to improve model interpretability.
- A targeted aggregation strategy is designed for fusing node and edge feature information: N-E aggregation. This strategy provides novel concepts for information aggregation in graph structures that encompass both node and edge features.

Property	Top-k Pool	SAG-Pool	Diff-Pool	ASAP	Ours
Sparse	✓	✓		✓	✓
Node aggregation			✓	✓	✓
Graph clustering			✓	✓	✓
Multidimensional edge feature support					✓

Table 1: Properties in Graph pooling methods

## Preliminaries

### Graph Definition and Feature Construction

FC is divided into static FC (sFC) and dynamic FC (dFC). dFC provides valuable information regarding the organization of functional brain networks that cannot be obtained by sFC (Díez-Cirarda et al. 2018), and dFC is more strongly associated with psychiatric disorder dysfunction (Espinoza et al. 2019). Therefore, dFC was selected in this study to describe the dynamic functional activities of the brain. Meanwhile, DSF-BrainNet (Zhu et al. 2023) was selected as the graph structure input for the GCN model.

DSF-BrainNet comprises two parts: node and edge features. Features are organized as time-series data, and both of which maintain the synchronization property. The fundamental notation is defined as follows:  $\mathcal{G} = (\mathcal{V}, \mathcal{E})$  denotes a graph, where  $\mathcal{V} = \{v_1, v_2, \dots, v_n\}$  denotes the set of brain region nodes and  $n$  denotes the number of nodes. Similarly,  $\mathcal{E} = \{(v_i, v_j)\}$  denotes the set of edges between graph nodes, where  $\mathcal{E}$  contains  $M$  elements. The function  $X: \mathcal{V} \mapsto \mathbb{R}^d$  assigns features to each node, and the function  $L: \mathcal{E} \mapsto \mathbb{R}^d$  assigns features to each edge. Thus,  $X(v_i), i = 1, 2, \dots, n$  is the feature vector of node  $v_i$ ;  $L(v_i, v_j)$  is the edge feature vector between nodes  $v_i, v_j$ .

For a node  $v_i$ , the set of its neighboring nodes is defined as  $Ne(v_i)$ , that is,  $Ne(v_i) = \{v_j | (v_i, v_j) \in \mathcal{E}\}$ , where  $v_j$  denotes the neighboring nodes of the  $v_i$ . In this study, it should be noted that the neighboring information of each node is stored in a matrix defined as  $A \in \mathbb{R}^{2 \times M}$ , where 2 indicates that

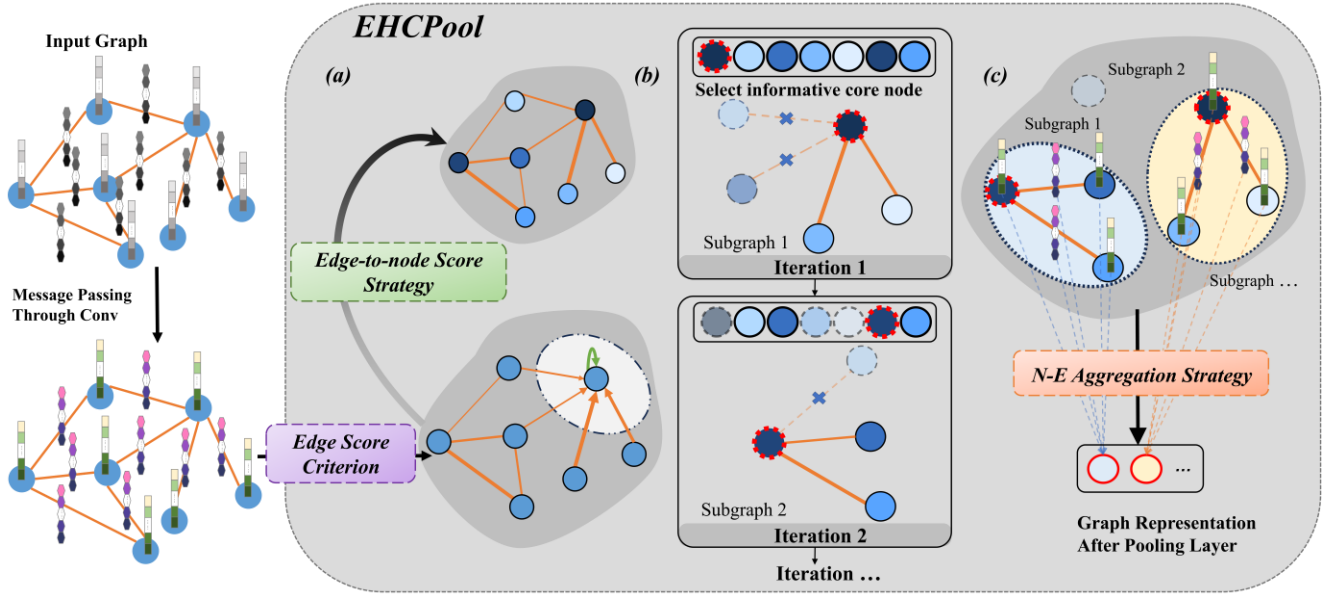


Figure 1: Overall EHCPool Architecture. Input graph constructed with multidimensional node and edge features is fed into the EHCPool for further representation learning after message passing through the convolutional layer. (a) Score calculation using edge feature information. The white dashed box shows the specific flow of the Edge-to-node strategy, where edge scores are depicted by edge thickness and node scores are depicted by the node color shade. (b) Cluster formation using an iterative hard clustering strategy. The outlined and highlighted node represents the most informative node within the current node set, i.e., the core node within the subgraph. After selecting core nodes, corresponding regular nodes are selected based on edge information scores. (c) Aggregate the core node vicinity information in each subgraph. The aggregated comprehensive information forms the basis vectors of each subgraph, which in turn form the EHCPool output.

$A$  has two feature dimensions: the first dimension is the index  $i$  of the initial node  $v_i$ , and the second is the index  $j$  of neighboring node  $v_j$ .  $M$  denotes the total number of edges in  $\mathcal{G} = (\mathcal{V}, \mathcal{E})$ . The specific computational procedure for node and edge feature construction is detailed in Appendix A.

## Graph Convolution Module

This study used Edge-Conditioned Convolution (ECC) (Simonovsky and Komodakis 2017) as the graph convolution module. Distinguishing from other traditional graph convolution methods, ECC is a generalized method that supports edge feature design, which is defined as follows:

$$X^l(v_i) = \frac{1}{|Ne(v_i)|} \sum_{v_j \in Ne(v_i)} F^l(L(v_i, v_j); w^l) X^{l-1}(v_j) + b^l \quad (1)$$

where  $l$  is the layer index in the feedforward neural network,  $b^l \in \mathbb{R}^{d_l}$  is a learnable bias and function  $F^l(\cdot)$  is a customized multilayer perceptron (MLP) that parameterized by learnable network weights  $w^l$ .

## EHCPool: Proposed Method

### Overall Architecture

To enhance the focus on edge feature information in the graph pooling, a hard clustering pooling method named

EHCPool is proposed. EHCPool is also designed to accommodate multidimensional edge features. As shown in Figure 1, EHCPool employs three novel sub-methods at its core, that is, (a) feature scoring strategy using ‘Edge-to-node’; (b) hard cluster formation using Iteration n-top; and (c) information aggregation using N-E aggregation.

### Edge-to-node score strategy

In existing graph pooling methods, a coarser subgraph is typically induced from the perspective of nodes, however, this ignores the essential role of edge features. Furthermore, for data problems in which the importance of edge feature information may be greater than that of the nodes, it is reasonable to emphasize the value of edge information during graph pooling. Therefore, in EHCPool, a criterion for calculating the edge feature information score was initially presented to evaluate the importance of the edge information, in which the edge feature information score  $\phi_e$  is expressed by the function  $F_{edges}(v_i, v_j)$ , and the set of all edge feature information scores is denoted by  $\phi_{edges} \in \mathbb{R}^M$ . This is implemented as follows:

$$F_{edges}(v_i, v_j) = \frac{L(v_i, v_j) p_l}{\|p_l\|_2} \quad (2)$$

$$\phi_{edges} = [\phi_{e_1}, \phi_{e_2}, \dots, \phi_{e_M}] \quad (3)$$

$$\hat{L}(v_i, v_j) = \hat{L}(v_i, v_j) \odot \sigma(F_{edges}(v_i, v_j)) \quad (4)$$

where  $\hat{L}(v_i, v_j) \in \mathbb{R}^{l_{ed}}$  is obtained from the edge features after message passing by the convolution module,  $p_1 \in \mathbb{R}^{d \times l}$  denotes the learnable projection vector.  $\|\cdot\|_2$  denotes the Euclidean distance ( $L_2$  norm).  $\hat{L}(v_i, v_j) \in \mathbb{R}^{l_{ed}}$  denotes the edge features after the scores are updated, ' $\odot$ ' is the (broadcasted) element-wise multiplication,  $\sigma(\cdot)$  represents the sigmoid activation function. Subsequently, we define a node feature information score strategy called 'Edge-to-node'. Noteworthy is that this strategy considers the importance of edge information without overlooking node information, in other words, it includes the scoring assessment of the core node and all its neighboring edges, which is an evaluation criterion that comprehensively considers both global and local representations. Similarly, the node feature information score  $\phi_i$  is expressed by the function  $F_{nodes}(v_i)$ , and the node feature information score set is expressed by  $\phi_{nodes} \in \mathbb{R}^n$ , which is implemented as follows:

$$F_{nodes}(v_i) = (1 - \delta) \frac{X'(v_i) p_2}{\|p_2\|_2} + \sum_{i=1}^{Ne(v_i)} \phi_i \quad (5)$$

$$\phi_{nodes} = [\phi_{v_1}, \phi_{v_2}, \dots, \phi_{v_n}] \quad (6)$$

where the hyperparameter  $\delta \in [0, 1]$  controls the extent to which node  $v_i$  is ignored, with a larger  $\delta$  indicating a higher level of node ignorance (generally defaults to 0).  $X'(v_i) \in \mathbb{R}^{l_{ed}}$  is obtained by passing the node features through the convolution module.  $p_2 \in \mathbb{R}^{d \times l}$  represents the learnable projection vector.

### Iteration n-top cluster strategy

Iteration n-top is a hard assignment with sparsity, which effectively reduces the computational complexity. Before clustering begins, two hyperparameters,  $\gamma$  and  $\beta$ , must be set in advance:  $\gamma$  controls the number of subgraphs (clusters) to be retained, and  $\beta$  controls the ratio of nodes retained in each subgraph. Considering one of the iterative processes as an example, first, based on the node feature information scores, the most informative node is considered the core node (cluster center) of the subgraph (cluster), as shown in Eq. (7):

$$idx_{max} = \arg \max_{v_i \in \mathcal{V}} (\phi_{nodes}) \quad (7)$$

where the function  $\arg \max(\cdot)$  is used to obtain the maximum value index  $idx_{max}$  in the set. Therefore, the index can be used to locate the core node  $v_{idx_{max}}$  in the subgraph, denoted as  $v_{Cnode}$ , and simultaneously, the set of neighboring edge indexes of this node is obtained in the adjacency matrix  $A$ , denoted as  $idx_{Nedges}$ . Next, the neighboring edges information scores are sorted, and subsequently, the neighboring nodes corresponding to the top  $(\lceil \beta n \rceil - 1)$  scoring edges are utilized as the regular nodes in the subgraph, and the edges from the regular nodes to the core nodes are retained as follows:

$$idx_{SortedEdges} = top\_rank(\phi_{idx_{Nedges}}, (\lceil \beta n \rceil - 1)) \quad (8)$$

$$idx_{Nenodes} = search\_A(idx_{SortedEdges}) \quad (9)$$

$$\mathcal{V}_{SubNodes} = \mathcal{V}_{idx_{Nnodes}}, \quad \mathcal{E}_{SubEdges} = \mathcal{E}_{idx_{SortedEdges}} \quad (10)$$

where  $top\_rank(\cdot)$  sorts the neighboring edges by edge scores and returns the top  $(\lceil \beta n \rceil - 1)$  indexes.  $search\_A(\cdot)$  uses the selected neighboring edge indexes  $idx_{SortedEdges}$  to obtain a set of neighboring node indexes corresponding to the given neighboring edges in the adjacency matrix  $A$ , denoted as  $idx_{Nenodes}$ .  $\mathcal{V}_{SubNodes} \subset \mathcal{V}$ , which is a subset of  $\mathcal{V}$ , contains regular nodes in the subgraph.  $\mathcal{E}_{SubEdges} \subset \mathcal{E}$ , which is a subset of  $\mathcal{E}$ , contains neighboring edges in the subgraph that are connected to regular nodes. Therefore, we define the subgraph dominated by the core node  $v_i$  as  $c(v_i) = \{v_j; (v_i, v_j) \in \mathcal{E}_{SubEdges}\} \cup \{v_i\}$ . Finally, the selected nodes are eliminated from the initial set of node feature information scores to obtain the updated node score set  $\phi_{update\_nodes}$ :

$$idx_{sub} = idx_{max} \cup idx_{Nenodes} \quad (11)$$

$$Z_{mask} = \Gamma_{idx_{sub}} \quad (12)$$

$$\phi_{update\_nodes} = \phi_{nodes} \odot Z_{mask} \quad (13)$$

where the symbol ' $\cup$ ' denotes the union operation,  $\Gamma_{idx_{sub}}$  denotes the index operation, and  $Z_{mask}$  denotes the feature mask (mask as 0). Hard cluster formation is completed, and the process is iterated until  $\gamma$  subgraphs  $c_k(v_i), k = 1, 2, \dots, \gamma$  are obtained.

### N-E Aggregation strategy

To target the representation learning of graph structures with both node and edge features, this study proposes a new information aggregation strategy called N-E Aggregation. This strategy performs independent information aggregation within each subgraph and can aggregate vicinity information (including nodes and edges) to the core nodes, thereby overcoming the defects of traditional graph pooling, which simply uses node updates and loses structural information. It also ensures the isolation of information interactions between subgraphs and avoids features redundancy and confusion. Once the aforementioned hard clustering process completes, the task here is to learn the subgraph representation by aggregating the regular nodes information  $v_j \in c_k(v_i)$  and the neighboring edges of each subgraph with its core node  $v_i$ . The aggregation process is as follows:

$$X''(v_i) = \sum_{v_j \in c_k(v_i)} Linear(L(v_i, v_j); w_c) X'(v_j) + b_c \quad (14)$$

where  $X''(v_i) \in \mathbb{R}^{l_{ed}}$  is the basis vector representing subgraph  $c_k(v_i)$  after information aggregation.  $w_c \in \mathbb{R}^{(d \times l_{ed}) \times l_{ed}}$  and  $b_c \in \mathbb{R}^{l_{ed}}$  denote the trainable weights and biases, respectively.  $Linear(\cdot)$  transforms edge feature vectors with the input dimensions of  $\mathbb{R}^{l_{ed}}$  into a weight matrix with the output dimensions of  $\mathbb{R}^{d \times l_{ed}}$ . Subsequently, this weight matrix is matrix-multiplied by the node feature vector  $X'(v_j)$  to obtain

Model	Type	COBRE+UCLA (mean (std), %)				REST-meta-MDD (mean (std), %)			
		ACC	SEN	SPE	F1-Score	ACC	SEN	SPE	F1-Score
SVM (V. Vapnik 1998)	sFC	70.62 (4.93)	69.72 (9.42)	71.20 (10.07)	67.05 (9.93)	72.52 (5.62)	71.91 (7.25)	70.42 (9.44)	69.94 (8.19)
GAT-LI (Hu, J. et al. 2021)	sFC	72.90 (5.85)	74.70 (9.63)	72.92 (10.34)	71.48 (8.91)	75.38 (6.13)	73.66 (8.07)	75.03 (8.56)	74.61 (9.52)
BrainGNN (X. Li et al. 2021)	sFC	74.11 (7.21)	<b>75.99</b> (8.78)	71.78 (8.64)	72.62 (6.57)	77.94 (6.35)	76.08 (9.54)	<b>77.18</b> (8.01)	75.98 (7.16)
GCN (T. N. Kipf and M. Welling 2016)	dFC	71.42 (8.48)	72.13 (9.20)	70.74 (12.58)	70.15 (7.92)	73.86 (7.67)	71.42 (7.24)	72.94 (8.66)	71.25 (10.37)
SCNN (Ji, J., Chen, Z., & Yang, C. 2022)	dFC	72.28 (7.85)	72.83 (11.73)	71.15 (10.47)	71.59 (6.29)	74.72 (8.34)	72.37 (11.34)	74.23 (11.28)	73.08 (10.68)
HFCN (C. Pan et al. 2022)	dFC	73.84 (7.29)	70.52 (9.97)	74.52 (10.82)	70.48 (9.60)	76.16 (8.21)	77.84 (10.29)	72.46 (11.75)	74.59 (9.66)
CRNN (K. Lin, et al. 2022)	dFC	72.98 (6.83)	72.20 (9.02)	72.83 (10.79)	72.22 (8.11)	74.79 (7.34)	73.72 (8.71)	73.86 (10.61)	72.32 (9.57)
EHCPool(ours)	dFC	<b>75.14</b> (2.62)	73.57 (4.36)	<b>75.29</b> (5.25)	<b>74.10</b> (4.31)	<b>78.83</b> (3.02)	<b>79.64</b> (5.21)	76.29 (7.64)	<b>77.51</b> (4.39)

Table 2: Comparison of the classification performance with different brain SOTA models

n the information passed to core node  $v_i$  from the neighboring edges  $L(v_i, v_j)$  and the corresponding neighboring node  $v_j$ . The EHCPool algorithm is detailed in the Appendix B.

## Experiments

### Experiment Setting

**Datasets and Preprocessing** In this study, three public datasets were selected for model evaluation: the COBRE (Mayer et al. 2013), UCLA (Bilder et al. 2020), and REST-meta-MDD (Chen et al. 2022). The REST-meta-MDD dataset is a multi-site mixed dataset for major depressive disorder (MDD). Similarly, the COBRE and UCLA datasets were mixed as a schizophrenia (SZ) dataset to test the robustness of the model. The corresponding information and preprocessing steps are detailed in the Appendix C.

**Metrics** Four metrics were used to evaluate the performance of the model: accuracy (ACC), sensitivity (SEN), specificity (SPE), and the F1-Score.

**Baselines** The comparison experiments were divided into two parts. The first uses seven state-of-the-art (SOTA) models commonly or exclusively used for brain data for comparison. The second uses four generalized graph pooling methods for comparison. The best performance was achieved by tuning the hyperparameters. (i) Brain SOTA models: Support Vector Machine (SVM) (Vapnik 1998). Graph Attention Network based learning and interpreting method (GAT-LI) (Hu et al. 2021). Brain Graph Neural Network (BrainGNN) (Li et al. 2021). GCN (Kipf and Welling 2016). Convolutional Recurrent Neural Network (CRNN) (Lin et al. 2022). High-order functional connectivity network (HFCN) (Pan et al. 2022). Sparse Convolutional Neural Network (SCNN) (Ji, Chen, and Yang 2021). (ii) Graph pooling methods: Graph U-Nets (Top-kPool) (Gao and Ji 2019). Self-Attention Graph Pooling (SAGPool) (Lee, Lee, and Kang 2019). Edge Contraction Pooling (EdgePool) (Diehl

2019). Spectral clustering Graph Pooling (MincutPool) (Bianchi, Grattarola, and Alippi 2019). Description of the above models are detailed in the Appendix D.

### Model Parameters

The code for this study was implemented using PyTorch Geometric and experimented on a NVIDIA GeForce RTX 3080 Ti GPU with 12GB memory. The model was sequentially set up with 2 convolutional layers, one pooling layer, and finally flattened input to a MLP layer for a fully connected output. Batchnorm and a Rectified Linear Unit (ReLU) were used after each convolution, and the hidden layer MLP neurons were set to twice the number of input features plus one. The Adam solver (Kingma and Ba 2014) and binary cross entropy with logits loss were used, with an initial learning rate of 0.001 and an epoch of 500. Simultaneously, we set the window width  $W = 95$  and sliding step  $s = 10$  for the sliding time window. In COBRE+UCLA dataset, we set the number of subgraphs (clusters) to be retained in  $\gamma = 5$ , and the number of nodes to be retained in each subgraph  $\beta n = 3$ . In REST-meta-MDD dataset, we set the number of subgraphs (clusters) to be retained in  $\gamma = 4$ , and the number of nodes to be retained in each subgraph  $\beta n = 3$ . In addition, all comparison experiments were performed ten times with five-fold cross validation, and the average value of each metric was considered the result.

### Experiment Results

**Brain SOTA Models** As shown in Table 2, the proposed model achieves enhanced performance on the two multi-site datasets, and outperforms the other baseline methods, thus substantiating its robustness. Specifically, the SVM and GCN yielded the worst results. Among the models utilizing dFC features, namely SCNN, HFCN, and CRNN, their performance slightly trailed behind that of BrainGNN employing sFC features. In contrast, the proposed EHCPool model

Method	Type	COBRE+UCLA (mean (std), %)				REST-meta-MDD (mean (std), %)			
		ACC	SEN	SPE	F1-Score	ACC	SEN	SPE	F1-Score
Top-kPool (Gao and Ji 2019)	node	73.68 (2.80)	72.31 (10.48)	75.17 (10.72)	70.29 (8.96)	75.81 (3.15)	75.37 (9.49)	71.04 (11.94)	73.13 (10.36)
SAGPool (Lee, Lee, and Kang 2019)	node	71.18 (1.81)	67.06 (5.88)	74.75 (6.99)	70.46 (7.79)	74.47 (2.29)	72.96 (5.04)	73.23 (5.67)	72.87 (7.71)
EdgePool (Diehl 2019)	edge	67.56 (3.63)	65.62 (8.34)	62.05 (11.27)	64.19 (11.21)	70.19 (5.65)	66.95 (6.31)	69.54 (10.47)	68.94 (11.84)
MincutPool (Bianchi, Grattarola, and Alippi 2019)	edge	74.36 (3.13)	72.84 (4.31)	74.15 (6.72)	73.42 (7.44)	77.65 (4.72)	76.12 (4.56)	74.36 (5.88)	74.57 (8.45)
EHCPool (proposed model)	node+edge	<b>75.14</b> (2.62)	<b>73.57</b> (4.36)	<b>75.29</b> (5.25)	<b>74.10</b> (4.31)	<b>78.83</b> (3.02)	<b>79.64</b> (5.21)	<b>76.29</b> (7.64)	<b>77.51</b> (4.39)

Table 3: Classification performance comparison between different graph pooling methods

exhibited superior performance compared to BrainGNN. It is evident that despite dFC containing a greater amount of latent feature information yet to be explored than sFC, the potential for models utilizing dFC to outperform the SOTA sFC models can be realized only through the adoption of suitable analytical frameworks and methodologies.

**Graph Pooling Methods** As shown in Table 3, the proposed method outperforms other node or edge-only graph pooling operators with an average ACC improvement of 3.44%, 4.30% on the two multi-site datasets, respectively. Because no common graph pooling method exists that computes edge scores based on edge features, e.g., EdgePool (Diehl 2019) and MincutPool (Bianchi, Grattarola, and Alippi 2019) both use node feature information to compute edge scores and do not accommodate multidimensional edge features, whereas EHCPool leverages multidimensional edge features to compute edge scores. This may explain why EHCPool is superior.

### Ablation Study

To evaluate the contribution of different sub-methods used in the proposed EHCPool model, we conducted exhaustive ablation experiments on two mixed datasets. (i) First, the scoring approach for node and edge features. Edge-to-node is a scoring strategy that systematically incorporates both

node and edge information, offering a holistic perspective. Therefore, we employed a local scoring strategy using only nodes and a global scoring strategy using only neighboring edges for replacement. (ii) Second, the graph pooling kernel for soft or hard clustering. Owing to the internal construction of Iteration n-top, it is not possible to implement soft clustering pooling within EHCPool, that is, direct replacement of Iteration n-top. Therefore, two SOTA soft cluster pooling methods, DiffPool and ASAP, were selected for ablation comparison. (iii) Third, the feature aggregation strategy. The two most representative graph pooling approaches were implemented for the direct replacement of N-E aggregation. Among these, Feature Selection is a strategy for directly selecting a portion of node features as the output, e.g., Top-kPool. Fully connected aggregation is a strategy for aggregating the node features within each cluster into the corresponding cluster basis vectors as output without considering the edge feature information, e.g., DiffPool and ASAP.

The results of the first set of experiments, as shown in Table 4, indicate that the Edge-to-node scoring strategy has better performance than the remaining two scoring strategies. This underscores the importance of integrated global and local representations in graph classification. The second set of experimental results, as shown in Table 5, further validate the superiority of the proposed method over alternative

Method	Type	COBRE+UCLA (mean (std), %)				REST-meta-MDD (mean (std), %)			
		ACC	SEN	SPE	F1-Score	ACC	SEN	SPE	F1-Score
Node-only features	local	73.14 (2.91)	72.47 (7.94)	72.83 (8.76)	70.30 (4.19)	76.41 (4.27)	75.44 (6.86)	75.03 (7.35)	75.62 (5.08)
Edge-only features	global	74.36 (5.61)	<b>74.57</b> (6.52)	73.22 (5.01)	72.34 (5.47)	77.56 (4.83)	78.81 (5.09)	75.74 (4.36)	75.28 (5.65)
Edge-to-node score strategy(ours)	local+global	<b>75.14</b> (2.62)	73.57 (4.36)	<b>75.29</b> (5.25)	<b>74.10</b> (4.31)	<b>78.83</b> (3.02)	<b>79.64</b> (5.21)	<b>76.29</b> (7.64)	<b>77.51</b> (4.39)

Table 4: Comparison between different feature scoring strategies in pooling kernel

Model	Clustering Type	COBRE+UCLA (mean (std), %)				REST-meta-MDD (mean (std), %)			
		ACC	SEN	SPE	F1-Score	ACC	SEN	SPE	F1-Score
DiffPool (Ying, R.et al 2018)	soft	74.42 (2.29)	70.68 (5.33)	74.73 (6.21)	70.94 (5.17)	77.78 (3.46)	76.81 (5.85)	<b>78.26</b> (4.91)	75.46 (6.83)
ASAP (Ranjan, E.et al 2019)	soft	70.31 (4.61)	69.55 (5.82)	73.61 (8.91)	66.36 (6.86)	76.72 (4.37)	77.52 (5.63)	74.49 (6.84)	75.34 (5.76)
Iteration n-top(ours)	hard	<b>75.14</b> (2.62)	<b>73.57</b> (4.36)	<b>75.29</b> (5.25)	<b>74.10</b> (4.31)	<b>78.83</b> (3.02)	<b>79.64</b> (5.21)	76.29 (7.64)	<b>77.51</b> (4.39)

Table 5: Different graph clustering pooling kernel comparison

Method	Type	COBRE+UCLA (mean (std), %)				REST-meta-MDD (mean (std), %)			
		ACC	SEN	SPE	F1-Score	ACC	SEN	SPE	F1-Score
Feature selection	-	70.29 (4.28)	71.25 (6.46)	70.40 (5.88)	69.82 (4.10)	74.15 (5.58)	72.61 (6.65)	74.33 (8.62)	73.06 (5.35)
Fully Connected aggregation	mix	74.84 (2.14)	<b>74.52</b> (7.73)	72.01 (8.59)	73.46 (5.95)	76.97 (3.71)	77.74 (6.71)	75.75 (6.86)	76.46 (5.66)
N-E Aggregation (ours)	independence	<b>75.14</b> (2.62)	73.57 (4.36)	<b>75.29</b> (5.25)	<b>74.10</b> (4.31)	<b>78.83</b> (3.02)	<b>79.64</b> (5.21)	<b>76.29</b> (7.64)	<b>77.51</b> (4.39)

Table 6: Comparison between different information aggregation strategies in pooling kernel

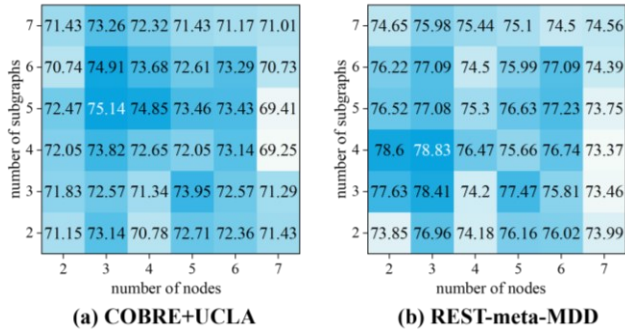


Figure 2: Discussion of  $\gamma$  and  $\beta$  parameters

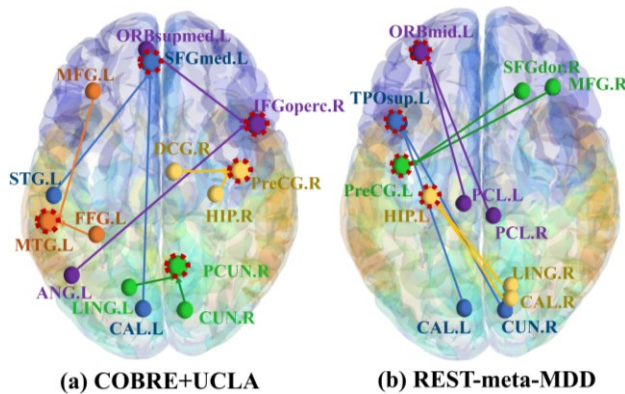


Figure 3: Proposed model subgraph division results and visualization at the highest accuracy. Different colors represent different subgraphs, outline highlighted nodes are core nodes. Full names of different brain regions are detailed in the Appendix E.

soft clustering graph pooling kernels. This suggests that the repeated representation of critical features in soft clustering may impact the experimental results. The third set of experimental results, as shown in Table 6, indicates that the performance of N-E aggregation surpasses that of the other methods. All the experimental findings mentioned above substantiate the efficacy of each respective sub-method.

### Sensitivity Analysis and Visualization

A sensitivity analysis was performed on the number of subgraphs (clusters) to be retained  $\gamma$  and the ratio of retained nodes per subgraph  $\beta$ . As shown in Figure 2, the model ac-

curacy is sensitive to these two hyperparameters, which indicates that multiple different types of abnormal functional brain networks (composed of different brain regions) may exist in psychiatric patients. It should be noted that is extremely difficult to probe various types of abnormal functional brain networks for psychiatric disorders from a data-driven perspective alone without using a priori knowledge. To the best of our knowledge, there is currently a lack of published deep learning investigations addressing this issue. Among the existing studies most pertinent to this topic, only BNC-DGHL (Ji and Zhang 2022) has simply combined the brain regions corresponding to the top 10 most abnormal FCs, treating them as a whole-brain abnormal functional network rather than exploring multiple different types of abnormal functional networks within the brain. However, as shown in Figure 3, and deduced from the results of the sensitivity analyses, it becomes evident that EHCPool exhibits the capacity to discern and categorize abnormal brain regions into different abnormal subgraphs, and thus to identify abnormal subnetworks in the brain that represent different types of functional abnormalities.

### Conclusion

This study proposes EHCPool, a clustering graph pooling method that supports multidimensional edge features. Specifically, the first ‘Edge-to-node’ score strategy for evaluating node significance based on edge features is presented, which improves the graph pooling representation learning capability. Subsequently, Iteration n-top is designed to perform adaptive hard clustering to capture critical subgraphs, which further exploits the application prospects of graph pooling methods and is expected to significantly improve interpretability of the model in specific scenarios. Finally, the proposed N-E Aggregation conducts an independent information aggregation in each subgraph, which provides a novel pooling aggregation concept for graph structures with both node and edge features. The superiority and robustness of EHCPool was validated in terms of its classification performance on two multi-site datasets. More meaningfully, EHCPool can be considered the first proposed method with the potential to explore different types of abnormal functional brain networks in deep learning research for the med-



ical imaging field. Future work will concentrate on constructing specialized datasets to probe abnormal functional brain networks in psychiatric patients using EHCPool.

## Acknowledgments

This work was supported in part by the grant from National Key R&D Program of China 2018YFA0701400; in part by the National Natural Science Foundation of China 61933003, U2033271; in part by the Science and Technology Project in Sichuan of China under grant 2022NSFSC0530, 2022NSFSC0507; in part by the Sichuan Provincial Program of Traditional Chinese Medicine of China under grant 2021ZD017; and in part by the Fundamental Research Funds for the Central Universities of China, Southwest Minzu University, under grant ZYN2023098.

## References

- Bianchi, F.M.; Grattarola, D.; and Alippi, C. 2019. Spectral Clustering with Graph Neural Networks for Graph Pooling. arXiv:1907.00481.
- Bifone, A.; Gozzi, A.; and Schwarz, A.J. 2010. Functional connectivity in the rat brain: a complex network approach. *Magnetic Resonance Imaging* 28(8):1200-1209. doi.org/10.1016/j.mri.2010.07.001.
- Bilder, R.; Poldrack, R.; Cannon, T.; London, E. Freimer, N.; Congdon, E.; Karlsgodt, K. and Sabb, F. 2020. UCLA Consortium for Neuropsychiatric Phenomics LA5c Study. Stanford Digital Repository. <http://purl.stanford.edu/mg599hw5271> and <https://openfmri.org/dataset/ds000030/>
- Chen, X.; Lu, B.; Li, H.X.; Li, X.Y.; Wang, Y.W.; Castellanos, F.X.; Cao, L.P.; Chen, N.X.; Chen, W.; Cheng, Y.Q.; Cui, S.X.; Deng, Z.Y.; Fang, Y.R.; Gong, Q.Y.; Guo, W.B.; Hu, Z.J.Y.; Kuang, L.; Li, B.J.; Li, L.; Li, T.; Lian, T.; Liao, Y.-F.; Liu, Y.S.; Liu, Z.N.; Lu, J.-P.; Luo, Q.H.; Meng, H.Q.; Peng, D.H.; Qiu, J.; Shen, Y.D.; Si, T.M.; Tang, Y.Q.; Wang, C.Y.; Wang, F.; Wang, H.N.; Wang, K.; Wang, X.; Wang, Y.; Wang, Z.H.; Wu, X.P.; Xie, C.M.; Xie, G.R.; Xie, P.; Xu, X.F.; Yang, H.; Yang, J.; Yao, S.Q.; Yu, Y.Q.; Yuan, Y.G.; Zhang, K.R.; Zhang, W.; Zhang, Z.J.; Zhu, J.J.; Zuo, X.N.; Zhao, J.P.; Zang, Y.F.; Consortium, T.D.; and Yan, C.G. 2022. The DIRECT consortium and the REST-meta-MDD project: towards neuroimaging biomarkers of major depressive disorder. *Psychoradiology* 2(1):32-42. doi.org/10.1093/psychrad/kkac005.
- D'souza, N.S.; Nebel, M.B.; Crocetti, D.; Robinson, J.; Mostofsky, S.H.; and Venkataraman, A. 2021. M-GCN: A Multimodal Graph Convolutional Network to Integrate Functional and Structural Connectomics Data to Predict Multidimensional Phenotypic Characterizations. *International Conference on Medical Imaging with Deep Learning*.
- Diehl, F. 2019. Edge Contraction Pooling for Graph Neural Networks. arXiv:1905.10990.
- Diez-Cirarda, M.; Strafella, A.P.; Kim, J.; Pena, J.; Ojeda, N.; Cabrera-Zubizarreta, A.; and Ibarretxe-Bilbao, N. 2018. Dynamic functional connectivity in Parkinson's disease patients with mild cognitive impairment and normal cognition. *Neuroimage-Clinical* 17:847-855. doi.org/10.1016/j.nicl.2017.12.013.
- Dong, Y.F.; Wang, Z.Q.; Du, J.P.; Fang, W.D.; and Li, L.H. 2023. Attention-based hierarchical denoised deep clustering network. *World Wide Web-Internet and Web Information Systems* 26(1):441-459. doi.org/10.1007/s11280-022-01007-4.
- Espinoza, F.A.; Liu, J.Y.; Ciarochi, J.; Turner, J.A.; Vergara, V.M.; Caprihan, A.; Misiura, M.; Johnson, H.J.; Long, J.D.; Bockholt, J.H.; Paulsen, J.S.; and Calhoun, V.D. 2019. Dynamic functional network connectivity in Huntington's disease and its associations with motor and cognitive measures. *Human Brain Mapping* 40(6):1955-1968. doi.org/10.1002/hbm.24504.
- Gao, H., and Ji, S. 2019. Graph u-nets. arXiv:1905.05178.
- Gopinath, K.; Desrosiers, C.; and Lombaert, H. 2022. Learnable Pooling in Graph Convolutional Networks for Brain Surface Analysis. *Ieee Transactions on Pattern Analysis and Machine Intelligence* 44(2):864-876. doi.org/10.1109/tpami.2020.3028391.
- He, X.; Wang, B.; Hu, Y.; Gao, J.; Sun, Y.; and Yin, B. 2022. Parallely Adaptive Graph Convolutional Clustering Model. *Ieee Transactions on Neural Networks and Learning Systems* PP (99):1-14. doi.org/10.1109/TNNLS.2022.3176411.
- Hu, J.L.; Cao, L.J.; Li, T.H.; Dong, S.B.; and Li, P. 2021. GAT-LI: a graph attention network based learning and interpreting method for functional brain network classification. *Bmc Bioinformatics* 22(1). doi.org/10.1186/s12859-021-04295-1.
- Huettel, S.A. 2012. Event-related fMRI in cognition. *Neuroimage* 62(2):1152-1156. doi.org/10.1016/j.neuroimage.2011.08.113.
- Ji, J.; Chen, Z.; and Yang, C. 2021. Convolutional Neural Network with Sparse Strategies to Classify Dynamic Functional Connectivity. *IEEE Journal of Biomedical and Health Informatics* 26(3):1219-1228. doi.org/10.1109/JBHI.2021.3100559.
- Ji, J., and Zhang, Y. 2022. Functional Brain Network Classification Based on Deep Graph Hashing Learning. *IEEE Transactions on Medical Imaging* 41(10):2891-2902. doi.org/10.1109/TMI.2022.3173428.
- Jiang, H.; Cao, P.; Xu, M.Y.; Yang, J.Z.; and Zaiane, O. 2020. Hi-GCN: A hierarchical graph convolution network for graph embedding learning of brain network and brain disorders prediction. *Computers in Biology and Medicine* 127. doi.org/10.1016/j.compbiomed.2020.104096.
- Kingma, D.P., and Ba, J. 2014. Adam: A Method for Stochastic Optimization. arXiv:1412.6980.
- Kipf, T., and Welling, M. 2016. Semi-Supervised Classification with Graph Convolutional Networks. arXiv:1609.02907.
- Klepl, D.; He, F.; Wu, M.; Blackburn, D.J.; and Sarrigiannis, P. 2022. EEG-Based Graph Neural Network Classification of Alzheimer's Disease: An Empirical Evaluation of Functional Connectivity Methods. *Ieee Transactions on Neural Systems and Rehabilitation Engineering* 30:2651-2660. doi.org/10.1109/tnsre.2022.3204913.
- Lee, J.; Lee, I.; and Kang, J. 2019. Self-Attention Graph Pooling. arXiv:1904.08082.
- Li, X.; Dvornek, N.C.; Zhou, Y.; Zhuang, J.; Ventola, P.; and Duncan, J.S. 2019. Graph Neural Network for Interpreting Task-fMRI Biomarkers. arXiv:1907.01661.
- Li, X.X.; Zhou, Y.; Dvornek, N.; Zhang, M.H.; Gao, S.Y.; Zhuang, J.T.; Scheinost, D.; Staib, L.H.; Ventola, P.; and Duncan, J.S. 2021. BrainGNN: Interpretable Brain Graph Neural Network for fMRI Analysis. *Medical Image Analysis* 74. doi.org/10.1016/j.media.2021.102233.



- Lin, K.Y.; Jie, B.; Dong, P.; Ding, X.; Bian, W.; and Liu, M. 2022. Convolutional Recurrent Neural Network for Dynamic Functional MRI Analysis and Brain Disease Identification. *Frontiers in Neuroscience* 16. doi.org/10.3389/fnins.2022.933660.
- Lin, S.H.N.; Lin, G.H.; Tsai, P.J.; Hsu, A.L.; Lo, M.T.; Yang, A.C.; Lin, C.P.; and Wu, C.W.W. 2016. Sensitivity enhancement of task-evoked fMRI using ensemble empirical mode decomposition. *Journal of Neuroscience Methods* 258:56-66. doi.org/10.1016/j.jneumeth.2015.10.009.
- Mayer, A.R.; Ruhl, D.A.; Merideth, F.L.; Ling, J.M.; Hanlon, F.M.; Bustillo, J.R.; and Cañive, J.M. 2013. Functional imaging of the hemodynamic sensory gating response in schizophrenia. *Human Brain Mapping* 34(9):2302-2312. doi.org/10.1002/hbm.22065.
- Nili, M.; Esfahan, S.M.; Bagheri, Y.; Vahabie, A.H.; Sa-nayci, M.; Ertiaei, A.; Shirani, M.; Dehaqani, M.R.A.; and Rezayat, E. 2023. The variation of functional connectivity and activity before and after thalamotomy surgery (review). *Frontiers in Human Neuroscience* 17. doi.org/10.3389/fnhum.2023.1108888.
- Pan, C.; Yu, H.; Fei, X.; Zheng, X.; and Yu, R. 2022. Temporal-spatial dynamic functional connectivity analysis in schizophrenia classification. *Frontiers in Neuroscience* 16. doi.org/10.3389/fnins.2022.965937.
- Pitsik, E.N.; Maximenko, V.A.; Kurkin, S.A.; Sergeev, A.P.; Stoyanov, D.; Paunova, R.; Kandilarova, S.; Simeonova, D.; and Hramov, A.E. 2023. The topology of fMRI-based networks defines the performance of a graph neural network for the classification of patients with major depressive disorder. *Chaos Solitons & Fractals* 167. doi.org/10.1016/j.chaos.2022.113041.
- Ranjan, E.; Sanyal, S.; and Talukdar, P.P. 2019. ASAP: Adaptive Structure Aware Pooling for Learning Hierarchical Graph Representations. arXiv:1911.07979.
- Simonovsky, M., and Komodakis, N. 2017. Dynamic Edge-Conditioned Filters in Convolutional Neural Networks on Graphs. arXiv:1704.02901.
- Vapnik, V.N. 1998. The Support Vector Method of Function Estimation. In *Nonlinear Modeling*, edited by Johan, A.K.S., and Joos, V., 55-85. New York: Springer.
- Venkatapathy, S.; Votinov, M.; Wagels, L.; Kim, S.; Lee, M.; Habel, U.; Ra, I.H.; and Jo, H.G. 2023. Ensemble graph neural network model for classification of major depressive disorder using whole-brain functional connectivity. *Frontiers in Psychiatry* 14. doi.org/10.3389/fpsy.2023.1125339.
- Wagner, F.H.; Dalagnol, R.; Sanchez, A.H.; Hirye, M.C.M.; Favrichon, S.; Lee, J.H.; Mauceri, S.; Yang, Y.; and Saatchi, S. 2022. K-textures, a self-supervised hard clustering deep learning algorithm for satellite image segmentation. *Frontiers in Environmental Science* 10. doi.org/10.3389/fenvs.2022.946729.
- Wen, G.Q.; Cao, P.; Bao, H.W.; Yang, W.J.; Zheng, T.; and Zaiane, O. 2022. MVS-GCN: A prior brain structure learning-guided multi-view graph convolution network for autism spectrum disorder diagnosis. *Computers in Biology and Medicine* 142. doi.org/10.1016/j.combiomed.2022.105239.
- Ying, R.; You, J.; Morris, C.; Ren, X.; Hamilton, W.L.; and Leskovec, J. 2018. Hierarchical Graph Representation Learning with Differentiable Pooling. arXiv:1806.08804.
- Zhang, R.T.; Ma, X.L.; Zhan, J.M.; and Yao, Y.Y. 2023. 3WC-D: A feature distribution-based adaptive three-way clustering method. *Applied Intelligence* 53(12):15561-15579. doi.org/10.1007/s10489-022-04332-3.
- Zhang, Z.; Bu, J.; Ester, M.; Zhang, J.; Li, Z.; Yao, C.; Huifen, D.; Yu, Z.; and Wang, C. 2023. Hierarchical Multi-View Graph Pooling With Structure Learning. *Ieee Transactions on Knowledge and Data Engineering* 35(1):545-559. doi.org/10.1109/TKDE.2021.3090664.
- Zhu, C.; Tan, Y.; Yang, S.; Miao, J.; Zhu, J.; Huang, H.; Yao, D.; and Luo, C. 2023. Temporal Dynamic Synchronous Functional Brain Network for Schizophrenia Diagnosis and Lateralization Analysis. arXiv:2304.01347.